Towards the Fastest Kinetics and Highest Uptake of Post-Functionalized UiO-66 for Hg^{2+} Removal from Water

Iris Tsz Yan Lam[1], Yufei Yuan[1], Ki-Taek Bang[1], Seon-Jin Choi[2], Dong-Myeong Shin[3], Dong Lu[4], and Yoonseob Kim[1,*]

[1]Department of Chemical and Biological Engineering, The Hong Kong University of Science and Technology, Hong Kong SAR, China

[2]Division of Materials of Science and Engineering, Hanyang University, Seoul 04763, Republic of Korea

[3]Department of Mechanical Engineering, The University of Hong Kong, Pokfulam Road, Hong Kong SAR, China

[4]Centre for Engineering Materials and Reliability, Guangzhou HKUST Fok Ying Tung Research Institute, Guangzhou, 511458, China

*To whom correspondence should be addressed: yoonseobkim@ust.hk

Abstract

Recent advances in adsorbents have improved the removal of mercury ions from wastewater. Metal–organic frameworks (MOFs) have been increasingly used as adsorbents due to their high adsorption capacity and ability to adsorb various heavy metal ions. UiO-66 (Zr) MOFs are mainly used because they are highly stable in aqueous solutions. However, most functionalized UiO-66 materials are unable to achieve a high adsorption capacity because of the undesired reactions that occur during post-functionalization. Herein, we report a facile post-functionalization method to synthesize a MOF adsorbent with fully active amide- and thiol-functionalized chelating groups, termed UiO-66-A.T. UiO-66-A.T. was synthesized via a two-step reaction by crosslinking with a monomer containing a disulfide moiety, followed by disulfide cleavage to activate the thiol groups. UiO-66-A.T. removed Hg^{2+} from water with a maximum adsorption capacity of 691 mg g^{-}

[1] and a rate constant of 0.28 g mg^{-1} min^{-1} at pH 1. In a mixed solution containing 10 different heavy metal ions, UiO-66-A.T. has a Hg^{2+} selectivity of 99.4%, which is the highest reported to date. These results demonstrate the effectiveness of our design strategy for synthesizing purely defined MOFs to achieve the best Hg^{2+} removal performance to date among post-functionalized UiO-66-type MOF adsorbents.

Keywords: Metal–organic framework; UiO-66; Post-functionalization; Adsorption

Environmental degradation caused by human activities is threatening environmental sustainability. The disposal of electronics such as semiconductors and optoelectronics releases a large amount of heavy metal ions, which are known to be toxic and persist in the environment. Mercury can accumulate in the ecosystem and does not biodegrade over time. Even in small amounts, mercury can pose serious health concerns, such as Minamata disease.[1] The United States Environmental Protection Agency has set the drinking water standard for mercury at 2 ppb.[2] Thus, it is imperative to develop technologies to efficiently remove mercury ions from water.

Heavy metal ions can be removed from water by various methods, including chemical precipitation, coagulation, electrochemical treatment, biofiltration, and ion exchange. However, these methods have the disadvantages of high cost, high energy consumption, low efficiency, and low selectivity, and some may cause secondary pollution.[3] Adsorption is a simple and facile approach for removing heavy metal ions in water. It typically has a low cost and low energy consumption, as well as other advantages such as a high uptake capacity, fast kinetics, and good recyclability, making it suitable for removing heavy metal ions from water.[4] Different adsorbents such as activated carbon, zeolite, silica, and biomass have been utilized to remove heavy metal ions;[5] however, these traditional adsorbents have limited adsorption capacity, selectivity, and

recyclability. The low adsorption capacity is primarily due to the scarcity of adsorption sites on the adsorbent surface, and low selectivity arises from a lack of functional tunability. However, recent advances in adsorbents, including the use of highly porous and stable materials, have received significant attention.[6,7] For example, metal–organic frameworks (MOFs) and covalent organic frameworks (COFs) are porous and can be post-functionalized, which can lead to a higher adsorption capacity and selectivity toward specific heavy metal ions.[8-13] COFs are constructed through stable covalent bonds of different organic monomers. However, the COF framework is mostly composed of amine- and aldehyde-derivatized organic ligands.[14] In comparison, the topological combinations and permutations of metal nodes and organic linkers that can be achieved with MOFs are significantly greater than for COFs. Furthermore, MOFs have a larger surface area and remain stable over a wide range of pH and temperatures. According to hard–soft acid–base theory (HSAB), there is strong coordination between a hard Lewis acid (high-valent metal ions such as Zr^{4+}, Ti^{4+}, Al^{3+}, Cr^{3+}, and Fe^{3+}) and a hard Lewis base (carboxylate-based ligands), or between a soft Lewis acid (Fe^{2+}, Co^{2+}, Ni^{2+}, Mn^{2+}, and Zn^{2+}) and a soft Lewis base (azolate-based ligands). This coordination is strong enough to persist in high-temperature and extreme pH conditions.[15] High-valency metal–carboxylate frameworks demonstrate a stronger robustness in acids due to the low pK_a of carboxylic acids, while low-valency metal–azolate frameworks demonstrate a stronger robustness in bases.

High-valency metal–carboxylate-based MOFs are ideal candidates for the removal of heavy metal ions from water because metals will form metal hydroxide precipitates in basic, but not acidic, solutions. Among the high-valency metal–carboxylate frameworks, Zr-based MOFs are well-studied and widely used water-stable MOFs.[16] Thus, in this study, we used UiO-66-NH_2 MOFs[17] as substrates and then post-functionalized them to include amide and thiol groups, which are

electron-rich atoms that can effectively chelate a large number of heavy metal ions. Similar to thiols, the electron-rich amide groups can also chelate heavy metal ions.[21] Notably, the amide groups are easily functionalized to further enhance the adsorption performance. In previous studies, post-functionalization strategies have simply directly added chelating groups to the backbones of UiO-66-type MOFs.[15] For example, Zhao et al.[18] introduced 1,4-phthalaldehyde to UiO-66-NH_2, then grafted L-cysteine through the Schiff base reaction to obtain Cys-UiO-66. Chai et al.[19] used glutaraldehyde as a bridge and introduced 4,6-diamino-2-mercaptopyrimidine to UiO-66-NH_2 through the Schiff base reaction to yield UiO-66-DMP. Awad et al.[20] converted UiO-66-NH_2 into UIO-66-NCS using thiophosgene as a coupling agent, and then the isothiocyanate group of UIO-66-NCS was chelated with the primary amine groups of 2-imino-4-thioburit through nucleophilic addition to yield UIO-66-IT. Saleem et al.[21] synthesized UiO-66-NHC(S)NHMe by introducing thiourea functionality to UiO-66-NH_2. The advantages of directly adding chelating monomers to the backbone are simplicity and practicality. However, the monomers used in post-functionalization are nucleophilic or contain both nucleophilic and electrophilic moieties. Thus, the direct functionalization reactions often result in undesired crosslinking of the MOFs or lead to oligomeric forms of connected functional groups, which reduces the pore size and the number of chelating groups and thus decreases adsorption performance (Fig. 1).

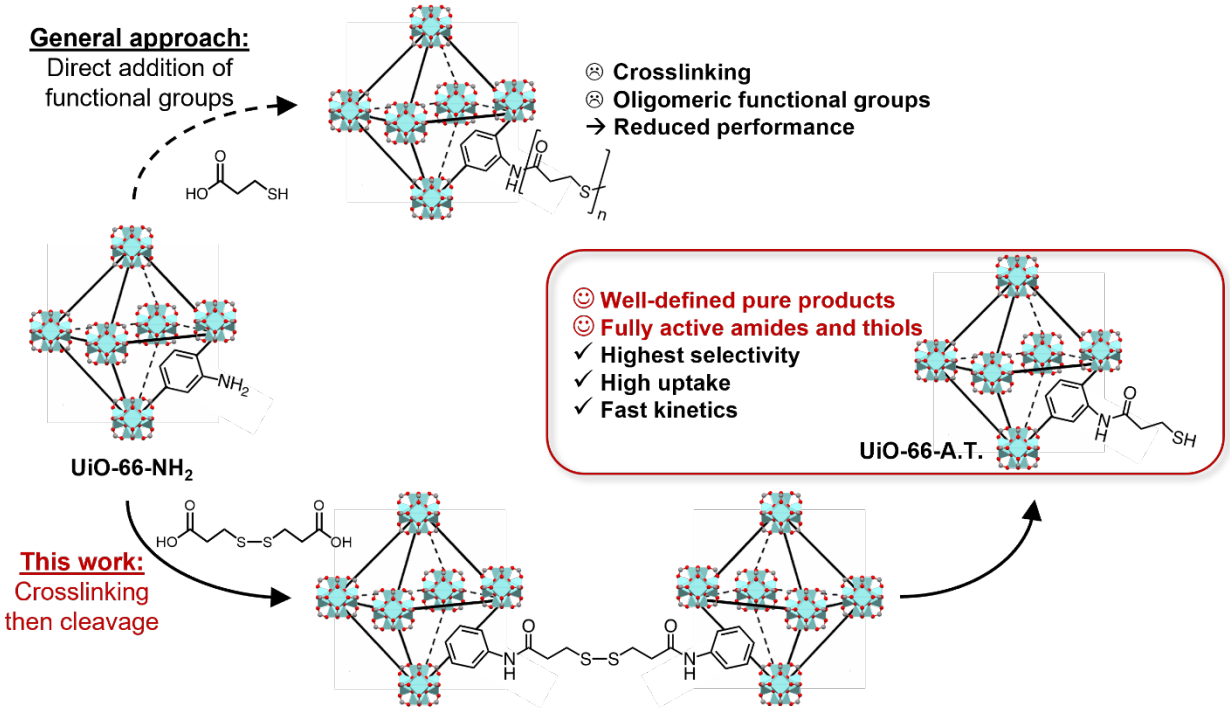

Figure 1. Concept and synthetic scheme of UiO-66-A.T. The synthesized UiO-66-NH_2 was coupled with 3,3′-dithiodipropionic acid, and the disulfide bonds were then cleaved by dithiothreitol. Oxygen, carbon, and zirconium are shown in red, gray, and light blue, respectively. Hydrogens are omitted in the Zr clusters.

To synthesize our MOF adsorbents, we initially planned to install 3-mercaptopropionic acid on the UiO-66-NH_2. However, if we used 3-mercaptopropionic acid to post-functionalize UiO-66-NH_2, oligomers or polymers containing thioester bonds could have formed through a condensation reaction, or the MOFs could have been crosslinked. One way to avoid these pitfalls is to use the solvent-assisted ligand exchange method, as described by Zhang et al.[22] However, the lower yield of the ligand exchange method would limit the uptake capacity, and the kinetics would remain average. To avoid these undesired reactions, we devised a system in which the MOFs were first crosslinked with a monomer containing a disulfide moiety. The crosslinking agent was then cleaved to expose a thiol group (Fig. 1). We used 3,3′-dithiodipropionic acid to crosslink UiO-66-NH_2 and then cleaved the disulfide bonds using dithiothreitol to activate the thiol groups (see the

supplementary information (SI) for experimental details). This cleavage was a clean reaction, as the S–S bond is weak and dithiothreitol is a strong reducing agent. As a result, the MOFs had purely defined and fully activated amide and thiol groups functionalized on the ligands. These well-defined pure products had fully active amides and thiols, which were expected to increase the adsorption performance regarding selectivity, uptake, and kinetics. With this design strategy, UiO-66 MOFs with amide and thiol groups (termed UiO-66-A.T.) were synthesized using UiO-66-NH_2 as the precursor (Fig. 1). The yields of the crosslinking and cleavage reactions were 78% and 81%, respectively (see the SI for the detailed conditions and digested NMR results). The ^{1}H NMR results confirmed that the reactions were successful (Fig. S1a, S1b, S1c, S1d). UiO-66-NH_2 displays three resonance peaks at 7.0, 7.2, and 7.7 ppm (Fig. S1b). These correspond to the protons on the benzene ring of 2-aminoterephthalic acid. These three aromatic peaks for UiO-66-A.T. were downshifted to 7.1, 7.2, and 7.7 ppm, respectively (Fig. S1d), and UiO-66-A.T. showed new peaks at 2.4 and 2.9 ppm, indicating that 3,3′-dithiodipropionic acid had been introduced into the MOF.

Both UiO-66-A.T. and UiO-66-NH_2 feature **fcu** topologies with $Zr_6(\mu_3\text{-}O)_4(\mu_3\text{-}OH)_4(COO)_{12}$ and Zr_6 clusters as secondary building units connected to 12 ditopic 2-aminoterephthalic acid (bdc-NH_2) linkers.[23,24] Scanning electron microscopy analysis showed that the as-synthesized UiO-66-A.T. and UiO-66-NH_2 had an octahedral morphology (Fig. 2a and S2). The edge length was 162 ± 30 nm (the measurements were performed in triplicate and averaged). The powder X-ray diffraction (PXRD) patterns of the as-synthesized UiO-66-A.T. and UiO-66-NH_2 demonstrated high crystallinity and were in agreement with the simulated diffraction patterns (Fig. 2b). The main diffraction peaks at approximately 7.4° and 8.5° were (010) and (011), respectively, which corresponds to the π-π stacking of the MOF ligands. The remaining diffraction peaks at approximately 12.0, 14.1, 14.7, 17.0, 20.9, 22.2, 25.7, 28.1, 30.7, 33.0, and 35.5°

correspond to the crystal facets (121), (120), (020), (022), (130), (030), (141), (344), (302), (151), and (051), respectively.

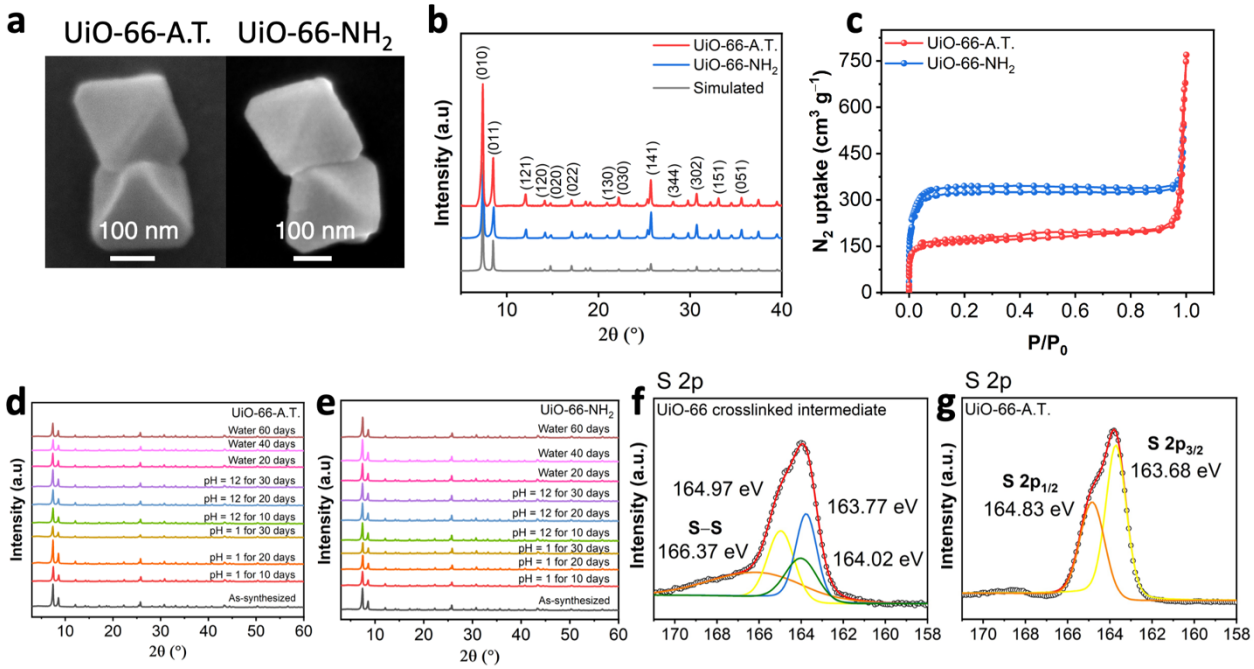

Figure 2. Characterization of the UiO-66 MOFs. a, Scanning electron microscopy image of UiO-66-A.T. and UiO-66-NH_2. **b,** PXRD patterns of simulation, UiO-66-A.T., and UiO-66-NH_2. **c,** Nitrogen adsorption isotherms of UiO-66-A.T. and UiO-66-NH_2. **d,** PXRD patterns of UiO-66-A.T. immersed in pH 1 and pH 12 for up to 30 days and immersed in water for up to 60 days. **e,** PXRD patterns of UiO-66-NH_2 immersed in pH 1 and pH 12 for up to 30 days and immersed in water for up to 60 days. **f,** XPS S 2p spectrum of the UiO-66 crosslinked intermediate. **g,** XPS S 2p spectrum of UiO-66-A.T.

Nitrogen adsorption/desorption isotherms measured at 77 K confirmed the synthesis of the highly porous MOFs (Fig. 2c). The calculated Brunauer–Emmett–Teller (BET) surface area, average pore size, and total pore volume of UiO-66-A.T. and UiO-66-NH_2 were 625 and 1318 m^2 g^{-1}, 23.9 and 50.7 Å, and 0.79 and 0.79 cm^3 g^{-1}, respectively (Fig. S3a). Due to the installation of the chelating groups occupying pore spaces, UiO-66-A.T. had a reduced BET surface area. After Hg^{2+} adsorption, the BET surface areas of UiO-66-A.T. and UiO-66-NH_2 were significantly reduced to 13 and 9 m^2 g^{-1}, respectively (Fig. S4a). Both UiO-66-A.T. and UiO-66-NH_2 possessed

high water and chemical stability (Fig. 2d, 2e). UiO-66-A.T. and UiO-66-NH_2 were immersed in water for 60 days, and the structures remained intact. Both were also immersed in pH 1 and 12 aqueous solutions for 30 days without losing any crystallinity. To evaluate whether deprotection was successfully carried out, the S 2p X-ray photoelectron spectroscopy (XPS) spectra of UiO-66-A.T. and the UiO-66 crosslinked intermediate were compared (Fig. 2f, 2g). The peak in the S 2p spectrum corresponding to the disulfide bonds was calculated to appear at a binding energy of 166.4 eV (Fig. 2f).[25] After deprotection, the binding energy of S 2p shifted toward a lower level, indicating that the disulfide bonds had been cleaved (Fig. 2g).[26] Elemental analysis using XPS showed a decreased sulfur content, also demonstrating that the disulfide bonds had been cleaved (Table S1).

Fourier-transform infrared spectroscopy and XPS also confirmed the growth of UiO-66-A.T. and UiO-66-NH_2 (Fig. S3c, S3d). In FTIR, the peaks at 1581 and 1680 cm^{-1} correspond to the Zr–OH bonds of UiO-66-A.T. and UiO-66-NH_2 (Fig. S3c). The broad peak located at 3433 cm^{-1} corresponds to the –OH bond in the carboxylic group of the ligand. The intensity of the peaks at 1398 cm^{-1} and 2931 cm^{-1} correspond to the C–C and C–H bonds, respectively. In XPS, two peaks in the Zr 3d spectrum for UiO-66.A.T. and UiO-66-NH_2 were fitted at 183.0 and 185.3 eV, 182.78 and 185.18 eV, respectively, which correspond to Zr $3d_{5/2}$ and Zr $3d_{3/2}$, respectively (Fig. S5d, S7d). Thermalgravimetric analysis showed that the synthesized MOFs had high thermal stability (Fig. S3e). The initial rapid weight loss of approximately 7% at 240 °C could be ascribed to the loss of residual solvent molecules. The subsequent weight loss around 240 and 350 °C was associated with linker decomposition. The frameworks survived until approximately 440 °C. The post-functionalized MOFs demonstrated higher thermal stability compared with MOFs that were not

functionalized. At 200 °C, both MOFs retained approximately 96% of their weight. At 700 °C, UiO-66-A.T. retained 46.3% of its weight, while UiO-66-NH_2 retained 41.5% of its weight.

To further elucidate the adsorption mechanism of UiO-66-A.T., the Hg(II) adsorbed UiO-66-A.T. was analyzed through FTIR and XPS (Fig. S3c, S3d). In FTIR, The peak at 1380 cm^{-1} corresponding to Hg–S demonstrates that a significant portion of Hg^{2+} was adsorbed by the thiol groups (Fig. S3c).[27] In XPS, The binding energy of S 2p for UiO-66-A.T. were observed at 163.89 and 165.90 eV, which are assigned to S $2p_{3/2}$ and S $2p_{1/2}$, respectively (Fig. S5d). After mercury adsorption, the peaks shifted to 163.56 and 168.79 eV, respectively (Fig. S6d). The peak intensity also significantly increased, indicating that thiol groups chelated with mercury ions. Two peaks located at 101.4 of Hg $4f_{7/2}$ and 105.4 eV of Hg $4f_{5/2}$ were observed, indicating that mercury ions existed in a divalent state and were chelated by the amino and thiol groups of UiO-66-A.T. (Fig. S6f). The binding energy of N 1s showed a slight increment in binding energy from 400.10 to 400.24 eV, which suggests the chelation of mercury ions by amino groups is not as significant compared to thiol groups (Fig. S5b, S6b). Thiol groups are the most electron-rich group among other functional groups, hence demonstrating a strong affinity for chelating Hg(II). S and N-containing groups are the soft Lewis bases and mercury ions are soft Lewis acids. Therefore, according to HSAB theory, UiO-66-A.T. has a higher affinity towards Hg(II).

The effect of pH on Hg^{2+} adsorption was studied using 1000 ppm solution at varying pH (Fig. S4b). The removal efficiency is the highest at pH 1. As the pH increases, mercury ions form hydroxides in the form of $Hg(OH)^+$ or $Hg(OH)_2$ and are difficult to be adsorbed. The maximum adsorption capacity is measured by performing adsorption tests at pH 1 using 1000 ppm Hg^{2+}, As(V) (AsO_4^{3-}), Cd^{2+}, Co^{2+}, Cu^{2+}, Zn^{2+}, Ni^{2+}, Pb^{2+}, Cr^{3+}, and Fe^{3+} single-metal stock solutions (Fig. 3a). The UiO-66-A.T. and UiO-66-NH_2 showed the highest adsorption capacity toward Hg^{2+} (691

± 13 and 208 ± 9 mg g^{-1}, respectively, Fig. 3a). UiO-66-A.T. and UiO-66-NH_2 showed poor adsorption of Cd^{2+}, As(V) (AsO_4^{3-}), Fe^{3+}, Cr^{3+}, and Co^{2+}, with adsorption capacities of 161, 98, 38, 29, and 15 mg g^{-1}, and 124, 119, 58, 45, and 38 mg g^{-1}, respectively. Both UiO-66-A.T. and UiO-66-NH_2 were barely active toward Cu^{2+}, Zn^{2+}, Ni^{2+}, and Pb^{2+}, with adsorption capacities of 0, 24, 28, and 0 mg g^{-1}, and 4.3, 4.3, 0.5, and 0 mg g^{-1}, respectively.

Selectivity tests were also performed to simulate contaminated water, as it usually contains multiple heavy metal ions. For this, both MOF adsorbents were soaked in a mixed-metal solution containing 1 mL each of 1000 ppm Hg^{2+}, As(V) (AsO_4^{3-}), Cd^{2+}, Co^{2+}, Cu^{2+}, Zn^{2+}, Ni^{2+}, Pb^{2+}, Cr^{3+}, and Fe^{3+} (Fig. 3b). UiO-66-A.T. showed the highest selectivity toward Hg^{2+}, with a removal rate of 99.4%, while UiO-66-NH_2 also showed high selectivity, with a removal rate of 75.9%. To the best of our knowledge, 99.4% Hg^{2+} removal is the highest reported for a UiO-66-based adsorbent. Our MOF adsorbents also removed As(V) (AsO_4^{3-}), Cd^{2+}, and Co^{2+}; however, the removal rates were low at 11.7%, 3.3%, and 0.4% for UiO-66-A.T., and 16.7%, 6.5%, and 3.5% for UiO-66-NH_2, respectively. The Hg^{2+} adsorption capacity of the UiO-66 crosslinked intermediate was 557 mg g^{-1} (Fig. 3c). The adsorption capacities of UiO-66-NH_2 and UiO-66-A.T. were measured in a concentration series made from a Hg^{2+} single-metal-ion stock solution (Fig. 3d).

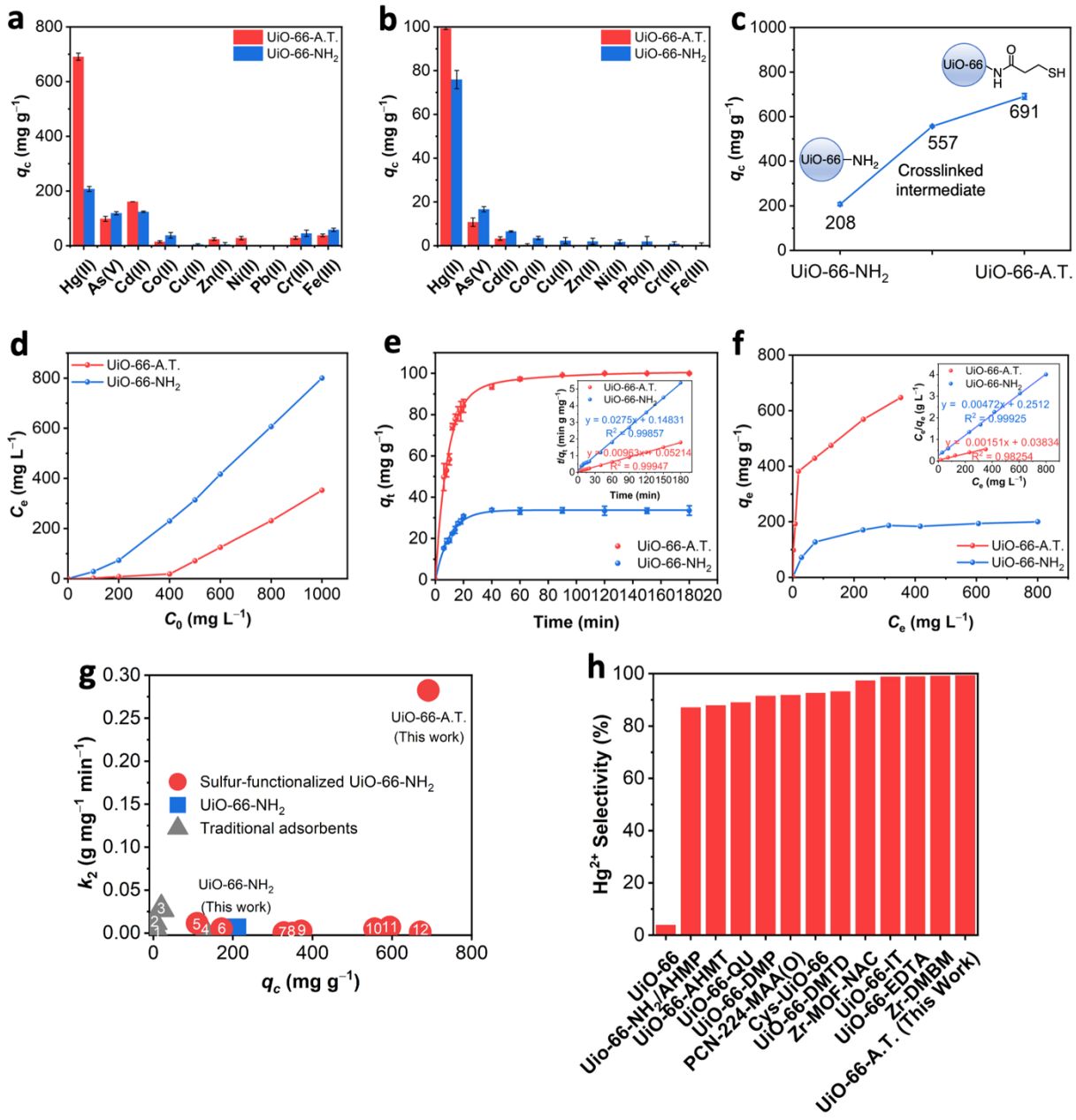

Figure 3. Adsorption performance of UiO-66-A.T. and UiO-66-NH$_2$. a, Adsorption capacity of the MOFs in single-metal ion solutions of 1000 ppm Hg^{2+}, As(V) (AsO_4^{3-}), Cd^{2+}, Co^{2+}, Cu^{2+}, Zn^{2+}, Ni^{2+}, Pb^{2+}, Cr^{3+}, and Fe^{3+} **b,** Adsorption capacity of MOFs in a mixed-metal solution containing 100 ppm each of Hg^{2+}, As(V) (AsO_4^{3-}), Cd^{2+}, Co^{2+}, Cu^{2+}, Zn^{2+}, Ni^{2+}, Pb^{2+}, Cr^{3+}, and Fe^{3+}. **c,** Amount of Hg^{2+} adsorbed by the MOFs. **d,** The equilibrium concentrations of Hg^{2+} after removing Hg^{2+} from different initial concentration stock solutions (100, 200, 400, 500, 600, 800, and 1000 ppm). **e,** Hg^{2+} adsorption kinetics in a 100 ppm Hg^{2+} solution containing the MOFs. The inset shows a pseudo-second-order fitting. **f,** Hg^{2+} adsorption isotherms of the MOFs. The inset shows

the linear regression by fitting the equilibrium adsorption data with the Langmuir adsorption model. **g,** Adsorption capacity and rate constant of traditional adsorbents and post-functionalized UiO-66-NH_2. 1: Zeolite,[40] 2: Activated carbon,[28] 3: Biomass,[29] 4: PTMS-functionalized silica gel,[30] 5: UiO-66-SH,[31] 6: Zr-DMBD,[32] 7: UiO-66-AHMT,[33] 8: Cys-UiO-66,[18] 9: UiO-66-EDTA,[34] 10: UiO-66-QU,[35] 11: Zr-MOF-NAC,[36] 12: UiO-66-DMTD,[37] This work: UiO-66-NH_2 and UiO-66-A.T. **h,** Hg^{2+} selectivity of post-functionalized UiO-66 MOFs. UiO-66,[21] Uio-66-NH_2/AHMP,[38] UiO-66-AHMT,[33] UiO-66-QU,[35] UiO-66-DMP,[19] PCN-224-MAA(O),[39] Cys-UiO-66,[18] UiO-66-DMTD,[37] Zr-MOF-NAC,[36] UiO-66-IT,[20] UiO-66-EDTA,[34] Zr-DMBM.[29]

The adsorption kinetics of the as-synthesized MOFs were measured in an aqueous solution of 100 ppm Hg^{2+} (Fig. 3e). Filtrate was collected at designated time intervals during 3 hours of magnetic stirring at room temperature. UiO-66-A.T. removed Hg^{2+} rapidly in the first 20 minutes (84.2% of Hg^{2+}) and achieved 100% removal in 120 minutes. UiO-66-NH_2 reached equilibrium in 60 minutes having removed 33.3% of Hg^{2+}. The adsorption kinetics data were fitted to a pseudo-first-order kinetic model (Eq. 1) and a pseudo-second-order kinetic model (Eq. 2) to describe the Hg^{2+} adsorption kinetics (Fig. S4c, 3e inset):

$$\ln(q_e - q_t) = \ln(q_e) - k_1 t \quad (Eq. 1)$$

$$\frac{t}{q_t} = \frac{1}{k_2 q_e^2} + \frac{t}{q_e} \quad (Eq. 2)$$

where q_t and q_e (in mg g^{-1}) are the amount of Hg^{2+} adsorbed at time t (in min) and at equilibrium, respectively. k_1 (in min^{-1}) and k_2 (in g mg^{-1} min^{-1}) are the rate constants of pseudo-first-order and pseudo-second-order adsorption, respectively. The maximum uptake capacity values of UiO-66-A.T. and UiO-66-NH_2 were calculated from the adsorption isotherms of the range of Hg^{2+} concentrations from 0 to 1000 mg L^{-1} (Fig. 3f). The adsorption isotherms were fitted to the Freundlich and Langmuir models (Fig. S4d, 3f inset). The experimental kinetic data conformed well to the pseudo-second-order model for the kinetics and the Langmuir model for the adsorption capacity (Fig. 3e inset, 3f inset). The correlation coefficients (R^2) of the pseudo-second-order

model for UiO-66-A.T. and UiO-66-NH_2 were 0.99893 and 0.99815, respectively. This suggests that chemisorption took place during the adsorption process, and a high density of adsorption sites chelated with the heavy metal ions.[40] The pseudo-second-order rate constants (k_2) for UiO-66-A.T. and UiO-66-NH_2 were 0.28 and 0.01 g mg^{-1} min^{-1}, respectively.

The adsorption performances of UiO-66-A.T. and UiO-66-NH_2 were compared with those of traditional adsorbents and other literature data (Fig. 3g). Notably, our UiO-66-A.T. showed the fastest adsorption behavior, with a k_2 of 0.28 g mg^{-1} min^{-1}, while the k_2 of UiO-66-NH_2 was 0.01 g mg^{-1} min^{-1}. The faster kinetics of UiO-66-A.T. was related to its larger surface area and fully active amide and thiol chelating groups. The uptake capacities of UiO-66-A.T. and UiO-66-NH_2 were 691 and 208 mg g^{-1}, respectively. As expected, the post-functionalized MOF showed a significantly improved uptake. The reported literature values for post-functionalized Zr-MOFs showed Hg^{2+} uptakes ranging from 110 to 671 mg g^{-1}, confirming that post-functionalized UiO-66 MOFs with more adsorption sites, such as amino (–NH_2), thiol (–SH), hydroxyl (–OH), carbonyl (C=O), and carboxyl (–COOH) sites, are more efficient at removing heavy metal ions. However, the previously reported k_2 values are very low, at 0.0001–0.0280 g mg^{-1} min^{-1}. This is presumably due to the undesired reactions mentioned above, such as crosslinking and oligomeric chelating groups (Fig. 1). Compared with the previously investigated materials, our UiO-66-A.T. had the highest adsorption capacity of 691 mg g^{-1} and the fastest kinetics (0.28 g mg^{-1} min^{-1}). This represents a significant advancement in adsorbent design and was realized because of the pure and well-defined amide and thiol chelating groups incorporated via the crosslinking and cleavage reactions, thus establishing a new design principle for post-functionalization. As a general comparison, the previously reported Hg^{2+} adsorption capacities for activated carbon, zeolite, biomass, and silica range from 2 to 210 mg g^{-1} (Table S2).[28,29,41] The literature value of UiO-66 for Hg^{2+} adsorption is 59 mg g^{-1},[37] and the values of other UiO-66-NH_2 derivatives for Hg^{2+}

adsorption are 103, 113, and 145 mg g^{-1} (Table S2).[18,33,37] For the Hg^{2+} selectivity, the reported values showed that unfunctionalized UiO-66 could have a Hg^{2+} selectivity of only 4%, while the post-functionalized material showed 87.9%–99.2% of Hg^{2+} selectivity. Nevertheless, our UiO-66-A.T. demonstrated the highest Hg^{2+} selectivity of 99.4% (Fig. 3h).

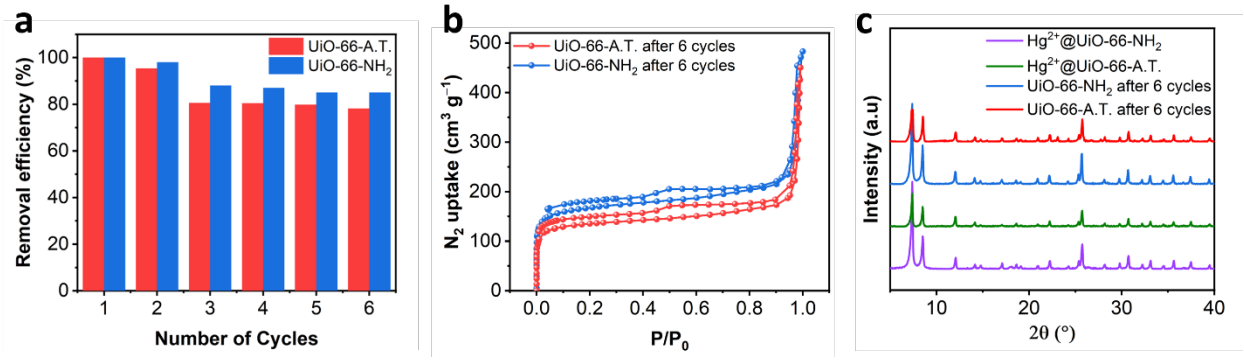

Figure 4. MOF adsorbent recyclability tests using Hg^{2+}. a, Removal efficiency after six adsorption–desorption cycles. **b,** Nitrogen adsorption isotherms of UiO-66-NH_2 and UiO-66-A.T. after six adsorption–desorption cycles. **c,** PXRD patterns of UiO-66-NH_2 and UiO-66-A.T. after six adsorption–desorption cycles.

We performed recyclability tests by putting the MOFs through six adsorption–desorption cycles (Fig. 4). Hg^{2+}-loaded UiO-66-A.T. and UiO-66-NH_2 were regenerated by treating them with 0.5 M HNO_3 and 1% thiourea solution. In the acidified thiourea solution, the thiourea is protonated by nitric acid and can then facilitate the desorption of Hg^{2+} that has adsorbed onto UiO-66-A.T. and UiO-66-NH_2.[37] Both UiO-66-A.T. and UiO-66-NH_2 demonstrated high recyclability, with removal rates of 78% and 85% after six cycles, respectively (Fig. 4a). The decreased removal rate may be attributable to residual heavy metal ions that had strongly bound to the MOFs. We then tested the BET surface area of UiO-66-A.T. and UiO-66-NH_2 after the six cycles, and they were measured to be 513 and 630 m^2 g^{-1}, respectively (Fig. S3b). The average pore size, and total pore volume of UiO-66-A.T. and UiO-66-NH_2 reduced to 18.7 and 43.7 Å, and 0.66 and 0.69 cm^3 g^{-1}, respectively (Fig. S3b). These results also indicated that some of the pores were blocked. The

PXRD patterns of UiO-66-A.T. and UiO-66-NH_2 after the six adsorption–desorption cycles remained intact (Fig. 4c), demonstrating that the morphology and chemical backbones persisted after the regeneration treatment.

Conclusion

We synthesized UiO-66-A.T., which was amide- and thiol-functionalized from UiO-66-NH_2. A two-step reaction was used to prepare the pure and well-defined amide and thiol functionalization via crosslinking and cleavage reactions. The developed process represents a significant advancement in Hg^{2+} adsorption. Compared with other UiO-66-based adsorbents, UiO-66-A.T. demonstrated a higher adsorption capacity and rate constant. UiO-66-A.T. removed Hg^{2+} with a maximum adsorption capacity of 691 mg g^{-1} and rate constant of 0.28 g mg^{-1} min^{-1}. In a mixed-metal solution, UiO-66-A.T. has the highest Hg^{2+} selectivity of 99.4% reported to date. Owing to its high performance, UiO-66-A.T. is a promising adsorbent for removing Hg^{2+} ions. Its high stability, capacity, selectivity, fast kinetics, and recyclability demonstrate the effectiveness of the crosslinking and cleavage strategy.

Acknowledgments

This work was supported by the Research Grants Council of the Hong Kong SAR Government (Early Career Scheme, #26309420, and General Research Fund, #16306921 and #16306022), Guangdong Provincial International Cooperation Program (Project number: 2021A0505033018), and the Department of Chemical and Biomolecular Engineering, HKUST (start-up funding).

Author Contributions

Y.K. conceived and supervised the project. S.J.C., D.M.S., and D.L. helped develop ideas and main schemes. I.T.Y.L designed and performed all the experiments and data analysis. Y.Y. helped with the characterization of MOFs. K.T.B. helped formulate the idea for the post-functionalization scheme. All authors discussed the results and contributed to the manuscript.

Conflict of interest

The authors declare no conflict of interest.

References

1. Tchounwou, P. B.; Yedjou, C. G.; Patlolla, A. K.; Sutton, D. J. Heavy Metal Toxicity and the Environment. In *Molecular, Clinical and Environmental Toxicology: Volume 3: Environmental Toxicology*; Luch, A., Ed.; Springer Basel: Basel, 2012; pp 133-164.

2. U.S. EPA. National Primary Drinking Water Regulations Mercury in Drinking-water Background document for development of WHO Guidelines for Drinking-water Quality.

3. Kumar, A.; Kim, Y.; Su, X.; Fukuda, H.; Naidu, G.; Du, F.; Vigneswaran, S.; Drioli, E.; Hatton, T. A.; Lienhard, J. H. Advances and challenges in metal ion separation from water. *Trends in Chemistry* **2021***, 3*, 819-831.

4. Yuan, Y.; Yu, J.; Chen, H.; Bang, K.; Pan, D.; Kim, Y. Thiol-functionalized Zr metal-organic frameworks for efficient removal of Fe^{3+} from water. *Cell Reports Physical Science* **2022***, 3*.

5. Foo, K. Y.; Hameed, B. H. The environmental applications of activated carbon/zeolite composite materials. *Adv. Colloid Interface Sci.* **2011***, 162*, 22-28.

6. Li, J.; Wang, X.; Zhao, G.; Chen, C.; Chai, Z.; Alsaedi, A.; Hayat, T.; Wang, X. Metal-organic framework-based materials: superior adsorbents for the capture of toxic and radioactive metal ions. *Chem. Soc. Rev.* **2018***, 47*, 2322-2356.

7. Sun, Q.; Aguila, B.; Perman, J.; Earl, L. D.; Abney, C. W.; Cheng, Y.; Wei, H.; Nguyen, N.; Wojtas, L.; Ma, S. Postsynthetically Modified Covalent Organic Frameworks for Efficient and Effective Mercury Removal. *J. Am. Chem. Soc* **2017***, 139*, 2786-2793.

8. Yuan, S.; Chen, Y.; Qin, J.; Lu, W.; Zou, L.; Zhang, Q.; Wang, X.; Sun, X.; Zhou, H. Linker Installation: Engineering Pore Environment with Precisely Placed Functionalities in Zirconium MOFs. *J. Am. Chem. Soc* **2016***, 138*, 8912-8919.

9. Eddaoudi, M.; Moler, D. B.; Li, H.; Chen, B.; Reineke, T. M.; O'Keeffe, M.; Yaghi, O. M. Modular Chemistry: Secondary Building Units as a Basis for the Design of Highly Porous and Robust Metal−Organic Carboxylate Frameworks. *Acc. Chem. Res.* **2001***, 34*, 319-330.

10. Furukawa, H.; Cordova, K. E.; O'Keeffe, M.; Yaghi, O. M. The Chemistry and Applications of Metal-Organic Frameworks. *Science* **2013***, 341*, 974.

11. Hao, M.; Liu, Y.; Wu, W.; Wang, S.; Yang, X.; Chen, Z.; Tang, Z.; Huang, Q.; Wang, S.; Yang, H.; Wang, X. Advanced porous adsorbents for radionuclides elimination. *EnergyChem* **2023**, 100101.

12. Liu, X.; Li, Y.; Chen, Z.; Yang, H.; Cai, Y.; Wang, S.; Chen, J.; Hu, B.; Huang, Q.; Shen, C.; Wang, X. Advanced porous nanomaterials as superior adsorbents for environmental pollutants removal from aqueous solutions. *Crit. Rev. Environ. Sci. Technol.* **2023***, 53*, 1289-1309.

13. Chen, Z.; Li, Y.; Cai, Y.; Wang, S.; Hu, B.; Li, B.; Ding, X.; Zhuang, L.; Wang, X. Application of covalent organic frameworks and metal–organic frameworks nanomaterials in organic/inorganic pollutants removal from solutions through sorption-catalysis strategies. *Carbon Research* **2023***, 2*, 8.

14. Feng, X.; Ding, X.; Jiang, D. Covalent organic frameworks. *Chem. Soc. Rev.* **2012***, 41*, 6010-6022.

15. Yuan, S.; Feng, L.; Wang, K.; Pang, J.; Bosch, M.; Lollar, C.; Sun, Y.; Qin, J.; Yang, X.; Zhang, P.; Wang, Q.; Zou, L.; Zhang, Y.; Zhang, L.; Fang, Y.; Li, J.; Zhou, H. Stable Metal–Organic Frameworks: Design, Synthesis, and Applications. *Adv. Mater.* **2018***, 30*.

16. Ahmadijokani, F.; Molavi, H.; Rezakazemi, M.; Tajahmadi, S.; Bahi, A.; Ko, F.; Aminabhavi, T. M.; Li, J.; Arjmand, M. UiO-66 metal–organic frameworks in water treatment: A critical review. *Progress in Materials Science* **2022***, 125*, 100904.

17. Wang, K.; Gu, J.; Yin, N. Efficient Removal of Pb(II) and Cd(II) Using NH_2-Functionalized Zr-MOFs via Rapid Microwave-Promoted Synthesis. *Ind. Eng. Chem. Res.* **2017***, 56*, 1880-1887.

18. Zhao, M.; Huang, Z.; Wang, S.; Zhang, L.; Zhou, Y. Design of l-Cysteine Functionalized UiO-66 MOFs for Selective Adsorption of Hg(II) in Aqueous Medium. *ACS Appl. Mater. Interfaces* **2019***, 11*, 46973.

19. Chai, X.; Dong, H.; Zhang, Z.; Qi, Z.; Chen, J.; Huang, Z.; Ye, C.; Qiu, T. A novel Zr-MOF modified by 4,6-Diamino-2-mercaptopyrimidine for exceptional Hg(II) removal. *Journal of Water Process Engineering* **2022***, 46*, 102606.

20. Awad, F. S.; Bakry, A. M.; Ibrahim, A. A.; Lin, A.; El-Shall, M. S. Thiol- and Amine-Incorporated UIO-66-NH_2 as an Efficient Adsorbent for the Removal of Mercury(II) and Phosphate Ions from Aqueous Solutions. *Ind. Eng. Chem. Res.* **2021***, 60*, 12675.

21. Saleem, H.; Rafique, U.; Davies, R. P. Investigations on post-synthetically modified UiO-66-NH_2 for the adsorptive removal of heavy metal ions from aqueous solution. *Microporous and Mesoporous Materials* **2016***, 221*, 238-244.

22. Zhang, L.; Wang, J.; Wang, H.; Zhang, W.; Zhu, W.; Du, T.; Ni, Y.; Xie, X.; Sun, J.; Wang, J. Rational design of smart adsorbent equipped with a sensitive indicator via ligand exchange: A hierarchical porous mixed-ligand MOF for simultaneous removal and detection of Hg^{2+}. *Nano Res* **2021***, 14*, 1523-1532.

23. DeStefano, M. R.; Islamoglu, T.; Garibay, S. J.; Hupp, J. T.; Farha, O. K. Room-Temperature Synthesis of UiO-66 and Thermal Modulation of Densities of Defect Sites. *Chem. Mater.* **2017***, 29*, 1357-1361.

24. Wang, H.; Dong, X.; Lin, J.; Teat, S. J.; Jensen, S.; Cure, J.; Alexandrov, E. V.; Xia, Q.; Tan, K.; Wang, Q.; Olson, D. H.; Proserpio, D. M.; Chabal, Y. J.; Thonhauser, T.; Sun, J.; Han, Y.; Li, J. Topologically guided tuning of Zr-MOF pore structures for highly selective separation of C6 alkane isomers. *Nat Commun* **2018***, 9*.

25. Mekaru, H.; Yoshigoe, A.; Nakamura, M.; Doura, T.; Tamanoi, F. Biodegradability of Disulfide-Organosilica Nanoparticles Evaluated by Soft X-ray Photoelectron Spectroscopy: Cancer Therapy Implications. *ACS Appl. Nano Mater.* **2018***, 2*, 479.

26. Huang, L.; Shen, R.; Liu, R.; Shuai, Q. Thiol-functionalized magnetic covalent organic frameworks by a cutting strategy for efficient removal of Hg^{2+} from water. *Journal of Hazardous Materials* **2020***, 392*, 122320.

27. Huang, L.; Shuai, Q. Facile Approach To Prepare Sulfur-Functionalized Magnetic Amide-Linked Organic Polymers for Enhanced Hg(II) Removal from Water. *ACS Sustainable Chem. Eng.* **2019***, 7*, 9957-9965.

28. Lu, X.; Jiang, J.; Sun, K.; Wang, J.; Zhang, Y. Influence of the pore structure and surface chemical properties of activated carbon on the adsorption of mercury from aqueous solutions. *Marine Pollution Bulletin* **2014***, 78*, 69-76.

29. Arias Arias, F. E.; Beneduci, A.; Chidichimo, F.; Furia, E.; Straface, S. Study of the adsorption of mercury (II) on lignocellulosic materials under static and dynamic conditions. *Chemosphere (Oxford)* **2017***, 180*, 11-23.

30. Najafi, M.; Rostamian, R.; Rafati, A. A. Chemically modified silica gel with thiol group as an adsorbent for retention of some toxic soft metal ions from water and industrial effluent. *Chem. Eng. J.* **2011***, 168*, 426-432.

31. Liu, F.; Xiong, W.; Feng, X.; Cheng, G.; Shi, L.; Chen, D.; Zhang, Y. Highly recyclable cysteamine-modified acid-resistant MOFs for enhancing Hg(II) removal from water. *Environ. Technol.* **2020***, 41*, 3094-3104.

32. Ding, L.; Luo, X.; Shao, P.; Yang, J.; Sun, D. Thiol-Functionalized Zr-Based Metal–Organic Framework for Capture of Hg(II) through a Proton Exchange Reaction. *ACS Sustainable Chem. Eng.* **2018***, 6*, 8494-8502.

33. Feng, L.; Zeng, T.; Hou, H. Post-functionalized metal−organic framework for effective and selective removal of Hg(II) in aqueous media. *Microporous and Mesoporous Materials* **2021***, 328*.

34. Wu, J.; Zhou, J.; Zhang, S.; Alsaedi, A.; Hayat, T.; Li, J.; Song, Y. Efficient removal of metal contaminants by EDTA modified MOF from aqueous solutions. *J. Colloid Interface Sci.* **2019***, 555*, 403-412.

35. Hu, Y.; Wang, S.; Zhang, L.; Yang, F. Selective removal of Hg(II) by UiO-66-NH_2 modified by 4-quinolinecarboxaldehyde: from experiment to mechanism. *Environmental Science and Pollution Research* **2023***, 30*, 2283-2297.

36. Lin, G.; Zeng, B.; Liu, X.; Li, J.; Zhang, B.; Zhang, L. Enhanced performance of functionalized MOF adsorbents for efficient removal of anthropogenic Hg(II) from water. *J. Clean. Prod.* **2022***, 381*, 134766.

37. Fu, L.; Wang, S.; Lin, G.; Zhang, L.; Liu, Q.; Fang, J.; Wei, C.; Liu, G. Post-functionalization of UiO-66-NH_2 by 2,5-Dimercapto-1,3,4-thiadiazole for the high efficient removal of Hg(II) in water. *Journal of Hazardous Materials* **2019***, 368*, 42-51.

38. Ruan, W.; Liu, H.; Qi, Y.; Zhou, M.; Wu, H.; Yang, H. Post-modification of Uio-66-NH_2 based on Schiff-base reaction for removal of Hg2+ from aqueous solution: Synthesis, adsorption performance and mechanism. *Fuel (Guildford)* **2022***, 319*, 123816.

39. Lin, D.; Liu, X.; Huang, R.; Qi, W.; Su, R.; He, Z. One-pot synthesis of mercapto functionalized Zr-MOFs for the enhanced removal of Hg^{2+} ions from water. *Chem.Commun.* **2019***, 55*, 6775-6778.

40. Hua, H.; Xiong, Y.; Fu, C.; Li, N. pH-sensitive membranes prepared with poly(methyl methacrylate) grafted poly(vinylidene fluoride) via ultraviolet irradiation-induced atom transfer radical polymerization. *RSC advances* **2014***, 4*, 39273-39279.

41. Fardmousavi, O.; Faghihian, H. Thiol-functionalized hierarchical zeolite nanocomposite for adsorption of Hg^{2+} from aqueous solutions. *Comptes Rendus Chimie* **2014***, 17*, 1203-1211.

TOC image

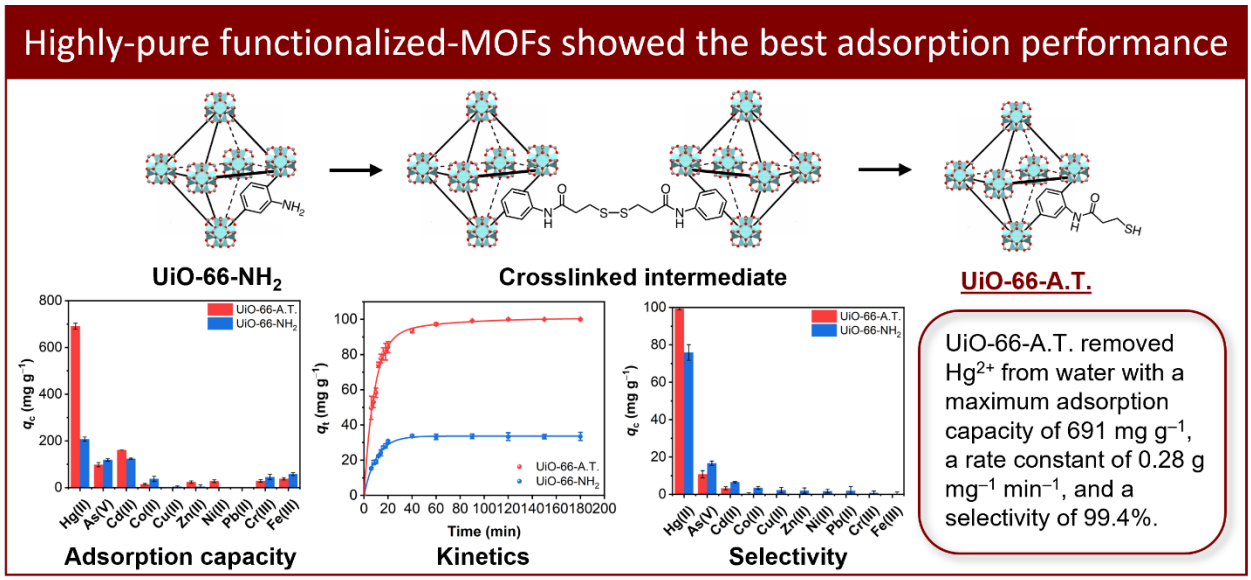
Highly-pure functionalized-MOFs showed the best adsorption performance
UiO-66-NH2
Crosslinked intermediate
UiO-66-A.T.
UiO-66-A.T.
UiO-66-NH2
Adsorption capacity
Kinetics
Time (min)
Selectivity
UiO-66-A.T. removed Hg2+ from water with a maximum adsorption capacity of 691 mg g−1, a rate constant of 0.28 g mg−1 min−1, and a selectivity of 99.4%.